ELSEVIER

Thermochimica Acta 303 (1997) 93–99

thermochimica acta

Behavior of ice–water transition in dimyristoylphosphatidylethanolamine–water system

Hiroshi Takahashi[a], Hiroyuki Aoki[b], Hideo Inoue[b], Michiko Kodama[b], Ichiro Hatta[a,*]

[a] *Department of Applied Physics, School of Engineering, Nagoya University Chikusa-ku, Nagoya, 464-01, Japan*
[b] *Department of Biochemistry, Faculty of Science, Okayama University of Science, 1-1, Ridai-cho, Okayama, 700, Japan*

Accepted 2 July 1997

Abstract

Differential scanning calorimetric (DSC) studies on the ice–water transition were performed for gel, metastable crystalline, and stable crystalline phases of a fully hydrated dimyristoylphosphatidylethanolamine (DMPE)–water system. We found that the ice-melting behavior differs among these three phases. Endothermic peaks due to the ice-melting were observed at temperatures below 0°C for the all phases. The starting temperature of ice-melting increases in the following order: gel (−35°C) < metastable crystalline (−20°C)< stable crystalline (−10°C) phases. The numbers of water molecules interacting with a DMPE headgroup were estimated to be 6, 7, and 2 for the gel, metastable crystalline and stable crystalline phases, respectively, from the transition enthalpies of the ice–water transitions. In addition, X-ray diffraction analyses revealed that the thickness of interlamellar water region is also different among the three phases and is less than ca. 0.8 nm for the all phases. Based on these results, the interaction of freezable bound water molecules and DMPE headgroups is discussed from the viewpoint of the relation between ice-melting temperatures and interbilayer hydration forces. © 1997 Elsevier Science B.V.

Keywords: DSC; Ice-melting; Lipid–water interaction; Phosphatidylethanolamine; X-ray diffraction

1. Introduction

Lipid bilayers are the fundamental structure of biomembranes [1], the physical and chemical properties of the lipid bilayers have, therefore, been widely studied by means of various techniques [2]. In these techniques, differential scanning calorimetry (DSC) is usually employed to investigate the phase behavior of the lipid bilayers [3–5]. In addition, DSC can be also applied for the studies of a lipid–water interaction, by measuring the ice-water transition of lipid–water systems [6]. Such DSC studies have been performed for synthetic phosphatidylcholine–water systems [7], galactosylcerebroside–water systems [8], central nerve myelin [9], etc. In these studies, the amount of nonfreezable water has been estimated from the plots of the transition enthalpies of the ice-melting at various levels of hydration. The results of these studies have revealed that the number of nonfreezable water molecules per lipid molecule depends on the type of lipid.

It is well known that lipid–water systems exhibit polymorphic behavior [10]. Judging from the fact that the arrangement of the headgroup is different in each phase, it is expected that the interaction of water and

*Corresponding author. Tel.: +81-52-789-4466; fax: +81-52-789-3724; e-mail: hatta@nuap.nagoya-u.ac.jp

PII S0040-6031(97)00252-9

the headgroups depends on the phases of the systems. However, there are a few studies [11,12] that prove this prediction on experimentally measuring the ice-water transition. The aim of this paper is to clarify the difference in the behavior of the ice-water transition, depending on the different phases. For this purpose, we performed DSC studies on the ice-melting for a fully hydrated dimyristoylphosphatidylethanolamine (DMPE)–water system. Our recent study [12] has revealed that the fully hydrated DMPE–water system adopts three different (gel, metastable crystalline, and stable crystalline) phases below the liquid–crystalline phase. In addition, a preliminary result revealed different behaviors of ice–water transitions for the gel and the stable crystalline phases [12].

In the present study, expanding the previous study [12], we investigated the behavior of ice–water transition for the three phases including the metastable crystalline phase. The amount of the water molecules interacting with DMPE molecules was calculated based on the transition enthalpy of the ice-melting. In addition to the DSC measurements, X-ray diffraction measurements were performed for the purpose of estimating the spacings of interlamellar water region for the three different phases. The diffraction data were analyzed by reconstructing an electron density profile for the gel phase and by calculating the Patterson function for both the crystalline phases. Based on both DSC and X-ray diffraction results, the interaction of water molecules with DMPE headgroups is discussed.

2. Experimental

2.1. Materials and sample preparation

1,2-Dimyristoyl-3-*sn*-phosphatidylethanolamine (DMPE) was purchased from Sigma (St. Louis, USA). The lipid was found to be at least 99% pure by thin-layer chromatography, therefore, it was used without further purification. To remove water molecules, the powder of DMPE was kept under high vacuum (10^{-4} Pa) and at room temperature for about three days. The crucible cell containing the dehydrated DMPE (ca. 50 mg) was sealed off in a dry box filled with dry N_2 gas and then weighed by a microbalance (Mettler M3, Switzerland). A fully hydrated sample of DMPE–water mixture at a water content of 25 wt% water (= 11.8 [H_2O]/[lipid]) was prepared by dropping a desired amount of water to the dehydrated lipid in the crucible cell, using a microsyringe. The water content was ascertained by weighing the sample and the cell. In a fully hydrated sample, the lamellar phase co-exists with excess bulk water. For the DMPE–water system in the gel phase, the excess water point has been estimated to be ca. 22 wt% (= 10 [H_2O]/[lipid]) on the basis of our preliminary calorimetric study [13]. For other phosphatidylethanolamine–water systems in the gel phase, the excess water points have been reported to be 12 to 18 wt% (= 6 to 9 [H_2O]/[lipid]) [14,15]. To achieve complete hydration and equilibration, all the samples were annealed by repeated thermal cycling at temperatures above and below the transition to the liquid–crystalline phase until the same DSC curve was obtained. The water contents were ascertained by weighing the sample and cell. For X-ray diffraction measurements, the samples were transferred to a capillary noted below.

2.2. Differential scanning calorimetry (DSC)

DSC measurements were carried out with a Mettler TA-4000 by using a high-pressure crucible. DSC scans were performed in the temperature range from −50°C to temperatures above the transition to the liquid–crystalline phase with a heating rate of 1.0°C/min.

2.3. X-ray diffraction

X-ray diffraction measurements were carried out by using a Ni-filtered CuK_α radiation source (RU200BEH, Rigaku, Tokyo, Japan) and a two-dimensional area detector (Imaging plate, Fuji Photo Film, Tokyo, Japan). An X-ray beam was focused with a double-mirror optical system. The sample was sealed in a fine-wall quartz capillary with 2 mm diameter. The capillary was fixed to a hollow brass holder. The temperature of the sample was controlled within ±0.1°C by circulating water from a temperature-controlled water bath (B. Braun, Melsungen, Germany) to the sample mount. The reading of the data on imaging plates was performed with a BAS2000 data reading system (Fuji Photo Film, Tokyo). The diffraction spacings were calibrated by

using the lamellar spacings of anhydrous cholesterol [16,17].

3. Results

3.1. Differential scanning calorimetry

Fig. 1 presents typical DSC curves in a (−40°)–(+80°)C temperature range for a fully hydrated DMPE–water sample (25 wt% H_2O). The DSC curve (a) in Fig. 1 was obtained by heating immediately after the sample was cooled from a liquid-crystalline phase temperature to −40°C. This sample adopts the gel phase at temperatures below 50°C, i.e. a sharp transition peak at 50°C ($\Delta H = 27.2$ kJ/mol) in the curve is due to the gel-to-liquid-crystalline phase transition. The DMPE–water system, following a low-temperature annealing treatment at −5°C for periods up to 30 days, gave rise to two lipid transition peaks at ca. 43 and 50°C (Fig. 1(b)). The low temperature transition peak at ca. 43°C ($\Delta H =$ 32.6 kJ/mol) is attributed to the transition from the metastable crystalline to the gel phases. The DSC curve (c) was obtained for the sample which was subjected to a two-stage annealing at different temperatures as follows; at first, the sample was maintained at ca. −50°C for several hours (nucleation) and then was kept at ca. 47°C for the same period (nuclear growth). The annealed sample gave rise to a transition peak at 56°C with a large enthalpy (80.8 kJ/mol) (Fig. 1(c)). The transition at 56°C is the stable crystalline-to-liquid-crystalline phase transition [12].

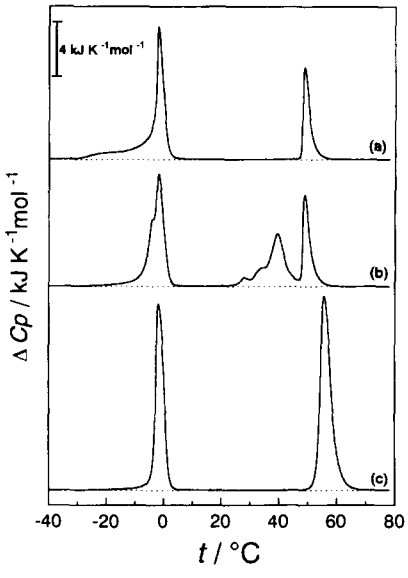

Fig. 1. Curves for DMPE–water system (25 wt% water) with various thermal histories: (a) scan without low-temperature storage; (b) scan after equilibration at −5°C for 30 days; and (c) scan after two-step annealing treatment (see text).

The endothermic peaks observed below 0°C are related to the ice–water transition. As shown in Fig. 1, the shapes of the DSC curve for the ice–water transition were also different among the three phases. For the gel phase sample, a broad anomaly of the heat capacity was observed from ca. −35°C (Fig. 1(a)). On the other hand, for the stable crystalline phase sample, the ice-melting curve begins to start from ca. −10°C (Fig. 1(c)). In the metastable crystalline phases, its ice-melting behavior is fairly different from those of the gel and stable crystalline phase. In addition to a normal ice-melting peak at 0°C, a sharp shoulder endothermic peak was observed at −5°C (Fig. 1(b)). The anomaly of the heat capacity was recognized from ca. −20°C in the DSC curve (Fig. 1(b)).

In the lipid–water systems, the ice–water transition observed at temperatures below 0°C originates from the water molecules interacting with lipid headgroups. In contrast, bulk free water molecules melt at 0°C. Therefore, the amount of bulk free water molecules can be calculated from the enthalpy change of the ice-melting peak at 0°C, by comparing with the enthalpy change (1.824 kJ/mol) of the hexagonal-ice-to-pure-water transition. To estimate the amount of bulk water molecules for the three phases, the ice-melting DSC curves were deconvoluted on the basis of a computer program attached to a Microcal calorimeter [18]. Results of the deconvolution analyses are shown in Fig. 2. As shown in Fig. 2(a), the ice-melting peak of the gel phases is deconvoluted into four components characterized by curves I, II, III, and IV. In contrast, the metastable crystalline phase lacks the deconvoluted curve I, while the stable crystalline phase lacks both the deconvoluted curves I and II. The corresponding deconvoluted curves in the three phases show nearly the same half-width and midpoint temperature. The deconvoluted curve IV at around 0°C corresponds to the ice-melting curve of the bulk free water. The amount of water molecules interacting with DMPE

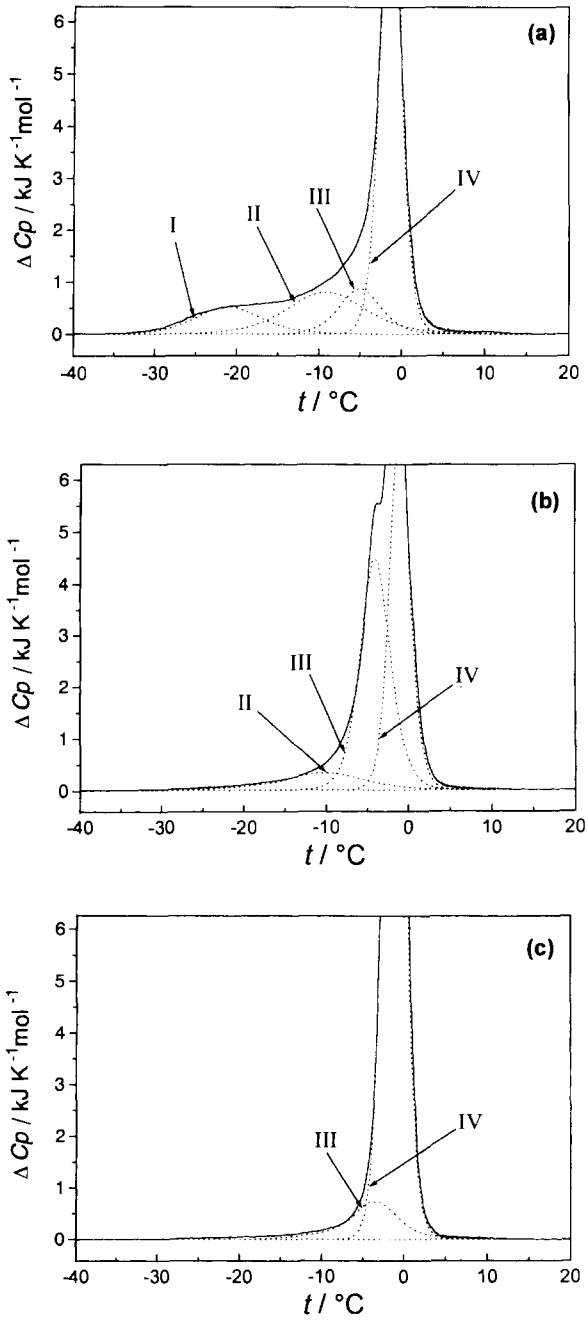

Fig. 2. Deconvolution analysis of ice-melting curves for (a) the gel, (b) metastable crystalline, and (c) the stable crystalline phases of the DMPE–water system (25 wt% water).

headgroups was estimated by subtracting the amount of bulk water molecules obtained by the deconvolution analysis from the total amount of water molecules (11.8 H_2O/lipid) for the 25 wt% water sample. Estimated numbers are 6, 7, and 2 water molecules per lipid for the gel, metastable crystalline and stable crystalline phases, respectively. These values are composed of freezable and nonfreezable water molecules interacting with headgroups.

3.2. X-ray diffraction

X-ray diffraction measurements were performed at 20°C for DMPE–water systems in the stable crystalline, the metastable crystalline, and the gel phases (the patterns not shown). The observed lamellar spacings were 5.68 ± 0.01 nm, 4.97 ± 0.01 nm, and 5.12 ± 0.01 nm for the gel, metastable crystalline, and stable crystalline phases, respectively. The lamellar reflections were observed up to the 6th, 10th and 14th orders for the gel, metastable crystalline, and stable crystalline phases, respectively. This result demonstrates that the phase with lower enthalpy gave rise to more reflection peaks.

In order to estimate the spacing of the interlamellar water region, we reconstructed the electron density profile for the gel phase from the lamellar intensity data. In general, it is difficult to determine the phase angles directly because, in principle, the possible combinations of the phase angles are infinite. However, if a system is centrosymmetric, the phase angles are restricted to either π or 0 [19]. Judging from the chemical structure, the DMPE–water multilamellar systems can be assumed to be centrosymmetric. Therefore, for the gel phase, it is enough to test 32 $(= 2^5)$ combinations of phase angles, because we obtained five intensity data for the lamellar reflections (the 5th order lamellar reflection could not be detected owing to its weak intensity). Examination of all possible phase combinations revealed that only one combination $(\pi, \pi, 0, \pi, -, \pi)$ gave rise to the electron density profile that is consistent with a bilayer structure, in which the origin is at the centre of the bilayers. This phase combination was also supported from the analysis by mean of a strip-function model [20,21]. The detailed analysis will be described elsewhere [13]. Fig. 3 displays the electron density profile of the gel phase DMPE–water system. In the profile, the highest peaks correspond to the positions of phosphorus atoms of the headgroups of the DMPE, because the heaviest atom in the system is a phosphorus atom. Therefore,

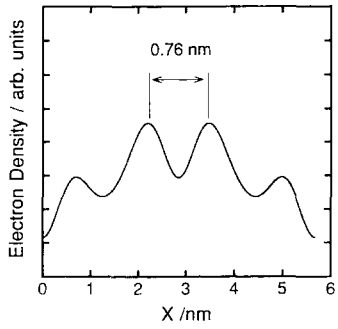

Fig. 3. One-dimensional electron density profile of the gel phase DMPE–water system at 20°C.

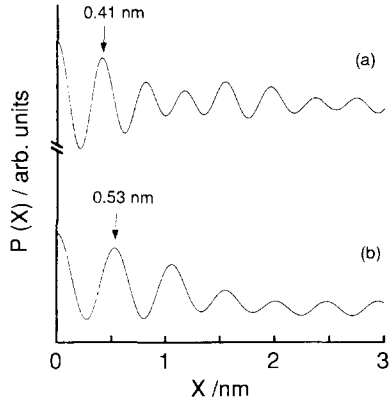

Fig. 4. One-dimensional Patterson function profiles of the (a) stable and (b) metastable crystalline phases of DMPE–water systems at 20°C. The positions indicated by arrows show the spacing of the phosphorus atoms in adjacent bilayers.

the spacing between the phosphorus atoms of the headgroup is estimated to be 0.76 nm.

For the metastable and stable crystalline phases, owing to a lot of lamellar reflections, it is impossible to determine their correct phases by means of direct methods. Therefore, we calculated the Patterson functions from the intensity data of lamellar reflections (Fig. 4). The Patterson function can be calculated without the information of the phase angle and it is an auto-correlation function of an electron density profile [19]. Therefore, the position of the highest peak, except for the origin in the Patterson function, corresponds to the spacing between the heaviest atoms in the unit cell. Thus, the spacing between the phosphorous atoms is found to be 0.53 and 0.41 nm, for the metastable and stable crystalline phase, respectively (Fig. 4).

For all the phases, the distance between the phosphorus atoms in the adjacent headgroups was determined. However, the necessary information is not this distance but the spacing of the interlamellar water region. Strictly speaking, this distance is not equal to the thickness of the water region, since the distinct boundary between the water layer and the lipid layer cannot be determined. A recent molecular dynamics simulation study on dilauroylphosphatidylethanolamine–water systems [22] has revealed that water molecules can penetrate into near glycerol backbones of the lipid bilayers and that over 90% of water molecules exist between the adjoining phosphate groups. Therefore, the distance between the phosphorus atoms is nearly equal to the thickness of the interlamellar water region.

4. Discussion

We estimated the amount of the water molecules interacting with DMPE headgroups for the three different phases from the present DSC results. However, the order of the number did not correspond to that of the thickness of the interlamellar water region estimated from the present X-ray diffraction data. That is, the thickness of the water layer for the gel phase is greater than that for the metastable crystalline phase. In contrast, the number (six) of the water molecules interacting with DMPE headgroups for the gel phase is smaller than that (seven) for the metastable crystalline phase. The discrepancy between the amount of water molecules and the thickness suggests that the surface area per lipid at the interface between the water layers and the lipid bilayers is different between the gel and metastable crystalline phases. The amount of the water molecules in the interlamellar region must be expressed not by the thickness of the water layer but by the volume of the water layer. The volume can be calculated from the product of the surface area and the thickness of the water layer. Hence, these results might indicate that the metastable crystalline phase has a larger area per lipid in comparison with the gel phase. The large surface area might be due to the tilt of the hydrocarbon chains towards the normal to the bilayer. In general,

the tilt of the hydrocarbon chains can simultaneously result in an increase of the surface area and a decrease of the bilayer thickness. Thus, the fact that the lamellar spacing of the metastable crystalline phase is smaller than that of other phases might be also explained in terms of the tilt of the hydrocarbon chains.

Let us consider the strength of the water–lipid interaction for each phase. Is the amount of water molecules interacting with DMPE headgroups proportional to the strength of the interaction? Does the large volume of the interlamellar water region mean the high strength of the interaction? It is well known that the thickness between adjacent bilayers is determined by the balance of various attractive and repulsive forces, van der Waals attractive force, electrostatic interaction, undulating force, hydration force, etc. [23]. Consequently, the amount of the interacting water molecules does not directly relate the strength of the interaction between the water molecules and lipid headgroups.

We will show that the ice-melting temperatures are related with the strength of the interaction. Prior to discussing the main subject, let us consider the possibility of an ice formation in the interlamellar water region. The present X-ray diffraction data showed that the thickness of water regions is less than ca. 0.8 nm for all phases. Thus, it is necessary to consider the ice formation in a small space. At temperature below 0°C, the ice phase is naturally a stable state; nevertheless, owing to the existence of the interfacial energy between ice and water, the ice nucleus does not always grow [24]. For a temperature $T(< 273\,\mathrm{K})$, the Gibbs free energy of condensation is given by

$$\Delta G_t = RT \ln\left(\frac{p_{\mathrm{ice}}}{p_{\mathrm{liquid}}}\right), \tag{1}$$

where, R is the gas constant and p_{ice} and p_{liquid} are the pressure of the sublimation of ice and the vapour pressure of supercooling water, respectively. Because there is a surface tension at the interface between the ice and the supercooling water, the net change of the Gibbs free energy associated with the formation of ice cluster with radius r is given by

$$\Delta G = 4\pi r^2\sigma + \frac{4}{3}\pi r^2 \Delta G_{\mathrm{t}}, \tag{2}$$

where σ is the interfacial free energy of the cluster. The critical radius for ice formation is obtained by setting the differential of Eq. (2) to zero, whence:

$$r^* = -\frac{2\sigma}{\Delta G_{\mathrm{t}}}. \tag{3}$$

Dufour and Defay [25] have estimated the critical radius at −50°C to be 0.83 nm, using Eq. (3). Judging from the results of the present X-ray diffraction (< ca.0.8 nm), the ice nucleus with the critical radii cannot grow in the interlamellar regions of the DMPE–water systems, i.e. no macroscopic ice crystal can exist in interlamellar region. As a result, it is expected that dehydration accompanying the ice formation causes a decrease of the distance between adjacent bilayers. Similar behavior of decreasing interlamellar spacings has been already reported for montmorillonite clay [26].

As Gleeson et al. [27] have pointed out, it can be assumed that the ice exists as a pool of crystalline ice in equilibrium with the freezable bound water associated with the lipid headgroups in the DMPE–water systems. Therefore, the ice-melting temperature is determined by the balance between the energy of hydration of the bilayers and that of the ice formation. The strength of hydration depends on that of the interaction between the bound water molecules and the lipid headgroups. In fact, the phenomena of the ice formation in multilamellar lipid–water systems has been discussed in the measurement of the hydration forces between lipid bilayers [27–29].

Next, let us consider the relationship between the melting temperature and the hydration force. In the interlamellar region of the lipid–water systems, the hydration force acts as a repulsion between the adjoining bilayers. The hydration force therefore provides the pressure to interlamellar water equilibrated with macroscopic ice at atmospheric pressure and temperatures below 0°C. Since the molar volume of water is smaller than that of ice, from the Clapeyron–Clausius equation, it can be concluded that the increase of the pressure reduces the ice-water transition temperature. In other words, the lower ice-melting temperature indicates the higher strength of the hydration force. Consequently, judging from the starting temperatures of the anomaly of the heat capacity (−35, −20, and −10°C for the gel, metastable crystalline, and stable crystalline phases, respectively) (Fig. 1), the strength of the lipid–water interaction can be considered to

increase in the order: stable crystalline < metastable crystalline < gel phases.

Acknowledgements

We gratefully acknowledge the High Intensity X-ray Diffraction Laboratory Execution Committee of Nagoya University for approval to use a BAS2000 system and also Mr. T. Hikage for his technical support for the BAS2000 system. This work is supported in part by Grant-in-aid from Ministry of Education, Science, Sports and Culture, Japan.

References

[1] S.J. Singer and G.L. Nicolson, Science, 175 (1972) 720.
[2] P.J. Quinn, The Molecular Biology of Cell Membranes, The Macmillan Press, London, 1976, Chap. 2.
[3] S. Mabrey and J.M. Sturtevant, Methods Membr. Biol., 9 (1978) 237.
[4] R.N. McElhaney, Chem. Phys. Lipids, 30 (1982) 229.
[5] R.L. Biltonen and D. Lichtenberg, Chem. Phys. Lipids, 64 (1993) 129.
[6] R.C. Warren, Physics and the Architecture of Cell Membranes, Adam Hilger, Briston, 1987, Chap. 5.
[7] D. Chapman and G.H. Dodd, in L.I. Rothfield (Ed. Structure and Function of Biological Membranes, Academic, Orland, 1971, p. 13–81.
[8] M.J. Ruocco and G.G. Shipley, Biochim. Biophys. Acta, 735 (1983) 305.
[9] B.D. Ladbrooke, T.J. Jenkinson and D. Chapman, Biochim. Biophys. Acta, 164 (1968) 101.
[10] I. Hatta, S. Kato and H. Takahashi, Phase Transitions, 45 (1993) 157.
[11] M. Kodama, H. Hashigami and S. Seki, J. Colloid Interface Sci., 117 (1987) 497.
[12] M. Kodama, H. Inoue and Y. Tsuchida, Thermochim. Acta, 266 (1995) 373.
[13] M. Kodama, H. Aoki, H. Takahashi and I. Hatta, Biochim. Biophys. Acta, in press.
[14] J.M. Seddon, G. Cevc, R.D. Kaye and D. Marsh, Biochemistry, 23 (1984) 2634.
[15] J.M. Seddon, J.H. Hogan, N.A. Warrender and E. Pabay-Peyroula, Progr. Colloid Polym. Sci., 81 (1990) 189.
[16] C.R. Loomis, G.G. Shipley and D.M. Small, J. Lipid Res., 20 (1979) 525.
[17] H.G. Shieh, L.G. Hoard and C.E. Nordman, Nature, 267 (1977) 287.
[18] C.W. Rigell, C.D. Saussure and E. Freire, Biochemistry, 24 (1985) 5638.
[19] D.W.L. Hukins, X-ray Diffraction by Disordered and Ordered Systems, Progamon Press, Oxford, 1981.
[20] C.R. Worthington, Biophys. J., 9 (1969) 222.
[21] P.J. Quinn, H. Takahashi and I. Hatta, Biophys. J., 68 (1995) 1374.
[22] K.V. Damodaran and K.M. Merz Jr., Langmuir, 9 (1993) 1179.
[23] G. Cevc and D. Marsh, Phospholipid Bilayers. Physical Principles and Models, Wiley, New York, 1987, Chaps. 3, 4, 5, and 8.
[24] F. Franks, Biophysics and Biochemistry at Low Temperatures, Cambridge University Press, Cambridge, 1985, Chap. 2.
[25] L. Dufour and R. Defay, Thermodynamics of Clouds, Academic Press, New York, 1963.
[26] D.M. Anderson, J. Colloid Interface Sci., 25 (1967) 174.
[27] J.T. Gleeson, S. Erramilli and S.M. Gruner, Biophys. J., 67 (1994) 706.
[28] J. Wolfe, Z. Yan and J.M. Pope, Biophys. Chem., 49 (1994) 51.
[29] Z. Yan, J. Pope and J. Wolfe, J. Chem. Soc. Faraday Trans., 89 (1993) 2583.